Probing nonstandard neutrino-electron interactions with solar and reactor neutrinos

A. Bolaños,[1] O. G. Miranda,[1] A. Palazzo,[2] M. A. Tórtola,[3] and J. W. F. Valle[2]

[1]*Departamento de Física, Centro de Investigación y de Estudios Avanzados del IPN, Apartado Postal 14-740 07000 México, D F, México*

[2]*AHEP Group, Institut de Física Corpuscular—C.S.I.C./Universitat de València, Edificio Institutos de Paterna, Apartado 22085, E-46071 Valencia, Spain*

[3]*II. Institut für theoretische Physik, Universität Hamburg, Luruper Chausee 149, 22761 Hamburg, Germany*

(Received 14 January 2009; published 24 June 2009)

Most neutrino mass extensions of the standard electroweak model entail nonstandard interactions which, in the low-energy limit, can be parametrized in term of effective four-fermion operators $\nu_\alpha \nu_\beta \bar{f} f$. Typically of subweak strength $\epsilon_{\alpha\beta} G_F$, these are characterized by dimensionless coupling parameters $\epsilon_{\alpha\beta}$, which may be relatively sizable in a wide class of schemes. Here we focus on nonuniversal flavor-conserving couplings ($\alpha = \beta$) with electrons ($f = e$) and analyze their impact on the phenomenology of solar neutrinos. We consistently take into account their effect both at the level of propagation, where they modify the standard Mikheev-Smirnov-Wolfenstein behavior, and at the level of detection, where they affect the cross section of neutrino elastic scattering on electrons. We find limits which are comparable to other existing model-independent constraints.

DOI: 10.1103/PhysRevD.79.113012 PACS numbers: 14.60.Pq, 13.15.+g

I. INTRODUCTION

Solar neutrino oscillations dominated by matter effects [1,2] are currently well established by solar neutrino experiments [3–22] and have been confirmed by the long-baseline KamLAND reactor experiment [23–25]. The combination between solar and KamLAND determines a unique solution in the mass-mixing parameter space, the so-called large mixing angle (LMA) solution; see, e.g., [26–29]. This solution has been shown to be quite robust against possible uncertainties in solar physics, such as magnetic fields in the radiative zone, that could give rise to noise fluctuations [30–37], as well as in the convective zone [38,39], that could induce spin-flavor neutrino conversions [40,41]. The KamLAND data play a crucial role in establishing that nonstandard effects can play only a subleading role [42], their amplitude being effectively constrained.

Altogether, the high precision and robustness of the current data render solar and reactor neutrinos a unique probe of possible physics beyond the standard model (SM) [42–48], complementing information from atmospheric and accelerator neutrinos [49,50]. Moreover, nonstandard interactions provide an important window of opportunity for current or upcoming long-baseline neutrino oscillation experiments and have been extensively considered in this framework [51–57].

It is worth stressing that, while constrained by the solar and KamLAND data, nonstandard interactions (NSI) provide an exception to robustness of the neutrino oscillation interpretation [45,46], and they might even shift the solution to the so-called dark side region of the neutrino parameter space [58]. Indeed, with oscillations still being the underlying mechanism, an additional degenerate oscillation solution in neutrino oscillation parameters can appear for sufficiently intense nonstandard interactions.

Neutrino NSI constitute an unavoidable feature of gauge models of neutrino mass, for example, models of the generic seesaw type [59] where neutrino masses arise from the admixture of isodoublet and isosinglet neutral leptons. In general, the lepton mixing matrix for charged currents is described by a matrix K, and the corresponding neutral weak interactions are described by a nontrivial matrix [59] $K^\dagger K$. In particular, in the simplest type-I seesaw schemes [60–63], the smallness of the neutrino mass implies that, barring fine-tuning, the magnitude of neutrino NSI and its effects are expected to be negligible. However, this need not be always the case. For example, by a suitable symmetry one may prevent the appearance of type-I seesaw mass contributions, hence allowing for the new neutral heavy leptons to lie at a mass scale accessible to accelerator experiments and, simultaneously, potentially produce sizable NSI strengths. For example, this may happen in some specially designed triplet (type-II) seesaw models [59,64], as shown in Ref. [65].

Alternatively, one may extend the lepton sector of the $SU(2) \otimes U(1)$ theory by adding a set of *two* 2-component isosinglet neutral fermions in each generation [66,67]. This scheme is sometimes called an "inverse seesaw" and provides an elegant way to generate small neutrino masses without a superheavy scale. This automatically allows for a sizable magnitude of neutrino NSI strengths, unconstrained by the smallness of neutrino masses.[1] The NSI which are engendered in this case will necessarily affect

[1]It also provides an explicit example for flavor and *CP* violation completely detached from the smallness of neutrino masses [68–70].

neutrino propagation properties in matter, an effect that may be resonant in certain cases [71–73]. They may also be large enough as to produce effects in the laboratory.

Another possible way to induce neutrino NSI is in the context of low-energy supersymmetry without R-parity conservation [74–77] of both the bilinear [78–81] and the trilinear type [82]. The smallness of neutrino masses may also follow from its radiative nature [83,84], allowing for possibly sizable NSI strengths.[2]

In general, one may consider a general class of nonstandard interactions described via the effective four-fermion Lagrangian

$$-\mathcal{L}^{\mathrm{eff}}_{\mathrm{NSI}} = \varepsilon^{fP}_{\alpha\beta} 2\sqrt{2} G_F (\bar{\nu}_\alpha \gamma_\rho L \nu_\beta)(\bar{f}\gamma^\rho P f), \qquad (1)$$

where G_F is the Fermi constant and $\varepsilon^{fP}_{\alpha\beta}$ parametrize the strength of the NSI. The chiral projectors P denote $\{R, L = (1 \pm \gamma^5)/2\}$, while α and β denote the three neutrino flavors, e, μ, and τ, and f is a first-generation SM fermion (e, u, or d).

For example, the existence of effective neutral current interactions contributing to the neutrino scattering off d quarks in matter provides new flavor-conserving as well as flavor-changing terms for the matter potentials of neutrinos. Such NSI are directly relevant for solar [46,58,87] and atmospheric neutrino propagation [49,50,88].

In general, the presence of NSI affects the solar neutrino phenomenology inducing profound modifications both in matter propagation [71,89,90] as well as in the detection process [43]. Although various works have investigated the effects of NSI at the level of propagation inside the Sun [45,46,58], the impact of NSI at the level of detection has received far less attention, and only qualitative studies have been performed so far [43,44].[3]

Therefore, it seems timely and interesting to investigate in more detail NSI trying to fill this gap in the literature. Our main aim is then to perform a quantitative analysis of the impact of NSI in solar neutrino phenomenology consistently taking into account their impact both on propagation and on detection processes. The simultaneous inclusion of NSI effects in both processes unavoidably renders the computational analysis very demanding since for each choice of the NSI couplings, one has to convolve the oscillation probability with the cross section of the relevant process. For definiteness in this work we have restricted our study to the following situation: (I) We have considered only nonuniversal (NU) flavor-conserving interactions neglecting flavor-changing neutral current interactions (FCNC). (II) We have considered interactions only with electrons ($f = e$). (III) We have performed our analysis switching on the interaction for one neutrino flavor at a time. (IV) We do not consider NSI of ν_μ with electrons since the current bounds in this case [48] $(-0.033 \le \varepsilon^L_{\mu\mu} \le 0.055,\ -0.040 \le \varepsilon^R_{\mu\mu} \le 0.053)$ are stronger than the attainable sensitivity from our solar analysis.

A final remark is in order. In general, one should also consider the possible simultaneous presence of FCNC and include NSI with up and/or down quarks.[4] We have not performed such a general analysis since the number of parameters would disproportionally increase. Although considering only flavor-preserving NSI with electrons may seem somewhat reductive, we deem that a model-indpendent detailed study of this specific case may provide particular insight and may be useful for future, more complete, studies.

The paper is organized as follows. In Sec. II, we discuss the impact of NU nonstandard interactions on propagation properties providing quantitative constraints on their amplitude. In Sec. III, we consider the effect of NSI on the elastic scattering cross section. In Sec. IV, we discuss the general case in which we simultaneously include NSI *both* in the propagation *and* in detection of electron neutrinos. In Sec. V, we show analogous results for the case of τ neutrinos. Finally, in Sec. VI, we trace our conclusions.

II. NONSTANDARD PROPAGATION

In this section we introduce the basic formalism describing neutrino propagation in the presence of nonstandard interactions and derive quantitative bounds on the amplitude of the effective nonuniversal couplings. These bounds will be an important ingredient to interpret the results of our full analysis presented in Secs. IV and V, where we consider the interplay of NSI effects in propagation and detection processes.

Here and in the following, we assume the standard parametrization for the lepton mixing matrix [59], within the convention adopted by the Particle Data Group [91], setting the small mixing angle θ_{13} to zero for the sake of simplicity. For $\theta_{13} = 0$, standard oscillations in the $\nu_e \to \nu_e$ channel probed by long-baseline reactor (KamLAND) and by solar neutrino experiments are driven by only two parameters: the mixing angle θ_{12} and the neutrino squared mass difference $\Delta m^2_{21} = m^2_2 - m^2_1$. In the flavor basis, the evolution of neutrinos can be written as

$$i\frac{d}{dx}\begin{pmatrix}\nu_e\\ \nu_a\end{pmatrix} = H\begin{pmatrix}\nu_e\\ \nu_a\end{pmatrix}, \qquad (2)$$

where ν_a is a linear superposition of ν_μ or ν_τ and H is the total Hamiltonian

$$H = H_{\mathrm{kin}} + H^{\mathrm{MSW}}_{\mathrm{dyn}} + H^{\mathrm{NSI}}_{\mathrm{dyn}} \qquad (3)$$

[2] For an alternative recent discussion of possible NSI strengths in a similar context, see Refs. [85,86]

[3] Solar and reactor neutrino fluxes are unaffected by the class of NSI which typically arise in models of neutrino mass.

[4] Limits on NSI involving up and down quarks have already been reported in the literature [49,50,58].

split as the sum of the kinetic term, the standard Mikheev-Smirnov-Wolfenstein (MSW) matter term [1,2] and of a new, NSI-induced, matter term [71]. The kinetic term depends on the mixing angle θ_{12}, on the squared mass difference $\Delta m^2_{21} = m^2_2 - m^2_1$, and on the energy E as

$$H_{\rm kin} = \frac{k}{2}\begin{pmatrix} -\cos 2\theta_{12} & \sin 2\theta_{12} \\ \sin 2\theta_{12} & \cos 2\theta_{12} \end{pmatrix}, \tag{4}$$

where $k = \Delta m^2_{21}/2E$ is the neutrino oscillation wave number. The standard (MSW) interaction term can be expressed as

$$H^{\rm MSW}_{\rm dyn} = V(x)\begin{pmatrix} 1 & 0 \\ 0 & 0 \end{pmatrix}, \tag{5}$$

where $V(x) = \sqrt{2}G_F N_e(x)$ is the effective potential induced by interaction with the electrons with number density $N_e(x)$. The NSI term can be cast in the form

$$H^{\rm NSI}_{\rm dyn} = V(x)\begin{pmatrix} 0 & \varepsilon \\ \varepsilon & \varepsilon' \end{pmatrix}, \tag{6}$$

where ε and ε' are two effective parameters that, neglecting $\varepsilon^{fP}_{\alpha\mu}$, are related with the vectorial couplings by

$$\varepsilon = -\sin\theta_{23}\varepsilon^{eV}_{e\tau}, \qquad \varepsilon' = \sin^2\theta_{23}\varepsilon^{eV}_{\tau\tau} - \varepsilon^{eV}_{ee}. \tag{7}$$

In the present work, we focus on the flavor-conserving NU couplings, setting the flavor-changing off-diagonal coupling $\varepsilon = 0$. Hence, in the treatment of solar neutrino propagation, in addition to the mass-mixing parameters we include the coupling ε'.

In our numerical analysis we have included the data from the radiochemical experiments Homestake [3], Sage [5], and GALLEX/GNO [6–8], from Super-KamioKande (Super-K) [10–12], from all three phases of the Sudbury Neutrino Observatory (SNO) [14–19], and from Borexino [21]. We have also included the latest KamLAND data [25] using a threshold of 2.6 MeV, which allows us to neglect the contribution of low-energy geoneutrinos.

It is worth noticing that, although we have incorporated both standard and nonstandard matter effects, due to the low matter density of the Earth's crust, they have only a negligible effect in KamLAND, for the range of parameters we are considering. Therefore the inclusion of KamLAND in the analysis has the important effect of determining the solar mass-mixing parameter, independently of the nonstandard interaction parameters.

In Fig. 1, we show the constraints we obtain on the parameter ε' from the solar neutrino data in combination with KamLAND after marginalization over the two mass-mixing parameters. We can qualitatively explain these bounds as follows. We notice that, since the term containing the effective NU coupling is diagonal, it is formally equivalent to a redefinition of the potential V[5]

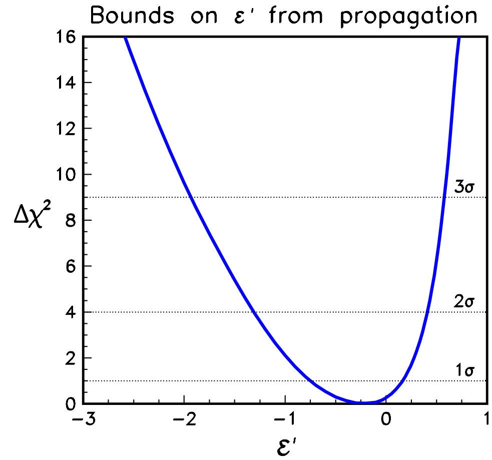

FIG. 1 (color online). Constraints on the effective amplitude characterizing NU nonstandard interactions in propagation.

$$V(x) \to (1 - \varepsilon')V(x). \tag{8}$$

In the LMA region the propagation is adiabatic so that, up to small Earth matter effects, the ν_e survival probability is given by the simple formula

$$P_{ee} = \tfrac{1}{2}(1 + \cos 2\tilde{\theta}_{12}(x_0)\cos 2\theta_{12}), \tag{9}$$

where $\tilde{\theta}_{12}(x_0)$ is the energy-dependent effective mixing angle in matter at the production point x_0 (see, e.g., [93] and references therein):

$$\cos 2\tilde{\theta}_{12}(x_0) = \frac{\cos 2\theta_{12} - V(x_0)/k}{\sqrt{(\cos 2\theta_{12} - V(x_0)/k)^2 + \sin^2 2\theta_{12}}}. \tag{10}$$

From the equations above we see that the survival probability depends on the potential $V(x)$ through the ratio V/k, and a rescaling of V can be compensated by a rescaling of the wave number k, which for a fixed neutrino energy implies a rescaling of the value of Δm^2_{21} preferred by data. Therefore, in the presence of a small NU coupling, the LMA solution moves upward ($\varepsilon' < 0$) or downward ($\varepsilon' > 0$) in the mass-mixing parameter space (not shown). Now we note that in the absence of nonstandard interactions the value of Δm^2_{21} preferred by solar data is in agreement to the one identified with high precision by KamLAND. Hence, the presence of the additional nonstandard effects tends to spoil this agreement, and the

[5]As shown in [92], the uncertainty in the solar composition leads to a small uncertainty on the electron neutrino density (and then on the potential V). In the region relevant for adiabatic transitions of solar neutrinos $R < 0.6$ (in units of solar radii), this can be quantified as less than 2% and hence is negligible in the context of our analysis.

tension arising between solar and KamLAND effectively constrains the amplitude of ε'.[6] It is interesting to note that the constraints on such a parameter have now reached the "sensitivity limit" attainable by KamLAND high precision measurements [25]. Indeed, we have checked that the constraints that one would obtain fixing the Δm^2_{21} at the best fit obtained by KamLAND are practically equivalent to those we obtain by exact marginalization. The freedom for ε' is essentially determined by the range of Δm^2_{21} allowed by the solar data *alone*. Indeed, by varying the value of ε', the wide solar LMA solution smoothly "slides" over the thin Δm^2_{21} region determined by KamLAND.

We observe that, while for small deviations around the standard value ($\varepsilon' = 0$) the bounds are symmetrical, for larger amplitudes the constraints becomes asymmetrical, i.e., stronger for positive values of ε'. This behavior is due to the typical shape of the solar LMA solution (see, for example, [26,28]) which is more (less) elongated towards large (low) Δm^2_{21} values. Indeed, the solar LMA solution is strongly limited from below by the (non)observation of day-night asymmetry in Super-K and SNO, and it is constrained in the upper part essentially by the charge current/neutral current (CC/NC) ratio measured by SNO. This asymmetric behavior will be relevant when considering (see Secs. IV and V) the interplay among the limits coming from nonstandard propagation with those coming from nonstandard detection.

III. NONSTANDARD DETECTION

Nonstandard couplings of neutrinos with electrons affect the elastic scattering ($\nu_a e \to \nu_a e$) process modifying the number of events and their spectral distribution expected in the Super-K detector and to a much lesser extent in the SNO detector. In principle, they also affect the Borexino spectrum, but we have checked that the current statistics is (still) too low to compete with Super-K.

The standard differential cross section for ($\nu_a e \to \nu_a e$) scattering processes has the well known form

$$\frac{d\sigma_a^{\rm std}}{dT}(E_\nu, T_e) = \frac{2G_F^2 m_e}{\pi}\left[(g_1^a)^2 + (g_2^a)^2\left(1 - \frac{T_e}{E_\nu}\right)^2 - g_1^a g_2^a \frac{m_e T_e}{E_\nu^2}\right], \tag{11}$$

where m_e is the electron mass, E_ν is the incident neutrino energy, and T_e is the electron recoil energy. The quantities g_1^a and g_2^a are related to the SM neutral current couplings of the electron $g_L^e = -1/2 + \sin^2\theta_W$ and $g_R^e = \sin^2\theta_W$, respectively, with $\sin^2\theta_W = 0.231\,19$ [91].[7] For $\nu_{\mu,\tau}$ neutrinos, which take part only in neutral current interactions, we have $g_1^{\mu,\tau} = g_L^e$ and $g_2^{\mu,\tau} = g_R^e$, while for electron neutrinos both CC and NC interactions are present and $g_1^e = 1 + g_L^e$, $g_2^e = g_R^e$. In the presence of NU nonstandard interactions, the cross section can be written in the same form of Eq. (11) but with $g^a_{1,2}$ replaced by the effective nonstandard couplings $\tilde{g}_1^a = g_1^a + \varepsilon_{aa}^{eL}$ and $\tilde{g}_2^a = g_2^a + \varepsilon_{aa}^{eR}$.

Strong limits can be placed on ν_μ interactions with electrons [48] ($-0.033 \le \varepsilon^L_{\mu\mu} \le 0.055$, $-0.040 \le \varepsilon^R_{\mu\mu} \le 0.053$). In contrast, the constraints on the other two NU couplings are rather loose [48]. Therefore in our analysis we can safely neglect NSI with muons of either helicity and focus in what follows on possible nonstandard couplings of ν_e and ν_τ. In addition, we have performed our analysis switching on one flavor nonstandard interaction at a time, due to computational limits. Indeed, already in this simple case we must consider as additional parameters ε_{aa}^{eL} as well as ε_{aa}^{eR} at the level of detection and their sum at the level of propagation.

Before introducing our numerical results, it is worth discussing the qualitative behavior one expects when NU interactions are present in the detection process. We first observe that for the high energy boron neutrinos (which are relevant for Super-K) MSW matter effects dominate and the survival probability is approximately $P_{ee} \sim \sin^2\theta_{12} \sim 1/3$. Furthermore, the transition probabilities to the other flavors are approximately equal ($P_{e\mu} \sim P_{e\tau} \sim 1/3$) since the admixture of ν_μ and ν_τ neutrinos is determined by the nearly maximal "atmospheric" mixing angle [26–29] ($\sin^2\theta_{23} \sim 0.5$). Hence, up to small Earth matter effects, an approximately equal admixture of the three neutrino flavors arrives at the Super-Kamiokande detector. Therefore from Eq. (11) one can expect the following general features: (I) In both cases of ν_e and ν_τ interactions, a deviation of the L-type coupling should mostly affect the total rate through the first term in Eq. (11). (II) The relative contribution of the first term in the cross section is almost 1 order of magnitude larger for ν_e compared to ν_τ [$(g_1^e)^2/(g_1^\tau)^2 \simeq 7$]. Thus we expect this feature to be reflected in a reduced sensitivity to $\varepsilon_{\tau\tau}^{eL}$ compared to ε_{ee}^{eL}. (III) Deviations of the R-type coupling will instead modify the expected energy spectrum through the second term and (to a lesser extent) through the third term. (IV) The value of g_2^a is identical for ν_e and ν_τ, and we expect comparable sensitivities for the ε_{ee}^{eR}, $\varepsilon_{\tau\tau}^{eR}$ effective couplings coming from the Super-K spectral information. (V) The third term (proportional to $g_1^a g_2^a$) is suppressed by the (energy-dependent) factor $m_e T_e/E_\nu^2$ and should induce non-negligible effects only in the case of electron neutrinos

[6] This behavior was indeed already noticed in Ref. [94], where upper bounds on possible deviations from the standard amplitude of the MSW interaction potential were considered.

[7] For our numerical analysis, instead of this simple tree level expression, we also include the radiative corrections given in Ref. [95].

($a = e$) since in this case g_1^a is bigger ($g_1^e \sim 0.73$ in the standard case).

IV. CONSTRAINTS ON ELECTRON NEUTRINO INTERACTIONS

In this section we present the numerical results of our analysis in the presence of NU couplings of ν_e with electrons. With this aim, we have performed a joint analysis of solar and KamLAND data in the $(\Delta m^2_{21}, \sin^2\theta_{12}, \varepsilon^{eL}_{ee}, \varepsilon^{eR}_{ee})$ parameter space, taking into account that only the vectorial combination $\varepsilon^{eV}_{ee} = \varepsilon^{eL}_{ee} + \varepsilon^{eR}_{ee}$ is involved in the propagation. Moreover, we have limited our scan in the L-type NSI parameter ε^{eL}_{ee} to the range $(-0.3, 0.3)$. Although a degeneracy in the value of this parameter appears when one includes only the νe scattering data [47], by allowing for NSI values as large as $\varepsilon^{eL}_{ee} = -1.5$, these values turn out to be forbidden when one also includes the LEP data, as shown in Ref. [48].

In the three panels of Fig. 2, we show the regions allowed in the plane $[\varepsilon^{eL}_{ee}, \varepsilon^{eR}_{ee}]$ where the mass-mixing parameters have been marginalized away. In the left panel, we show the region allowed when we switch on the nonstandard effects *only* in the detection process. The sensitivity to deviations of the L-type coupling is higher than the R-type sensitivity (notice the different scale used for the two parameters). This behavior follows from the fact that the most important effect of ε^{eL}_{ee} arises from the first term in Eq. (11) and approximately consists in an energy-independent rescaling of the cross section. This in turn leads to deviations of the predicted theoretical values of the total Super-K rate which are rejected by all of the remaining solar data. To better understand this point, we note that, if only Super-K data were included in the analysis, large deviations of the total cross section could be allowed since they could be compensated by a rescaling of the theoretical boron flux which is still uncertain at the $\sim$20% level. However, the combination of the Super-K data with the other solar neutrino experiments drastically improves the sensitivity to ε^{eL}_{ee}. In particular, SNO plays a crucial role in this respect, limiting possible departures of the total Super-K rate in two ways. First, the NC measurement provides a direct measurement of the boron flux in agreement with the SM prediction to within $\sim$6% or so, effectively reducing the allowed space for a possible rescaling of the boron flux. Second, the precision measurement of the SNO CC rate imposes a further constraint on the Super-K neutrino-electron scattering rate.

As already observed in the previous section, the constraints on the R-type coupling come from the spectral information obtained in the Super-K experiment. Current Super-K data are consistent with the spectrum predicted for a standard cross section while still allowing for appreciable deviations. Therefore the limits on the R-type coupling are looser compared with those obtained on the L-type one (note the different scale used for ε^{eR}_{ee} and ε^{eL}_{ee}). We observe that the "barycenter" of the allowed region is slightly shifted toward negative values of ε^{eR}_{ee} (~ -0.2). For such values the coefficient $g_2^e \sim 0$ and both the second and third (energy-dependent) terms in Eq. (11) tend to vanish indicating a slight preference of the data for an energy-independent cross section. We also observe how the allowed region is elongated towards negative values of both nonstandard L-type and R-type couplings indicating that in this region of the parameter space a degeneracy exists between the second and the third terms in Eq. (11). Indeed, the second term tends to give a negative tilt to the Super-K energy spectrum which is counterbalanced by the positive tilt induced by the third one (indeed, its coefficient is positive in this parameter region since g_2^e assumes negative values).

In the middle panel of Fig. 2, we report the constraints obtained when we include nonstandard effects only in neutrino propagation, as already discussed in Sec. II. In this plane these constraints are represented by diagonal bands delimited by lines corresponding to constant values of the vectorial coupling. This plot clearly shows how these constraints are different and complementary to those coming from detection.

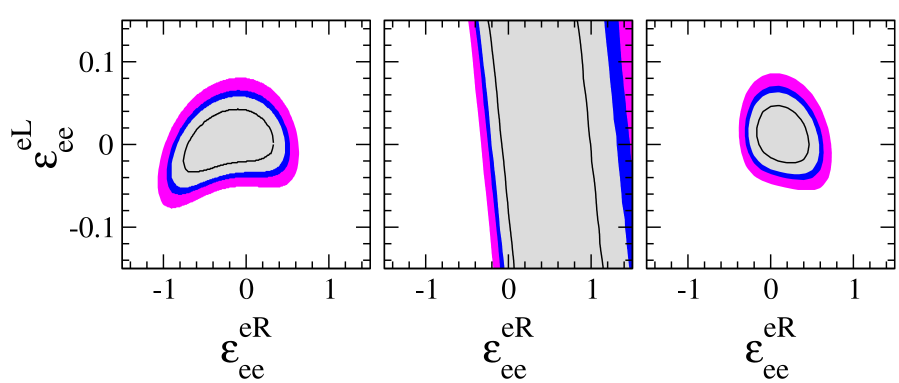

FIG. 2 (color online). Constraints on the electron neutrino nonstandard interactions. Bounds at 68%, 90%, 95%, and 99% for 2 d.o.f. In the left panel nonstandard effects are included only in the detection, in the middle panel only in propagation, and in the right panel the effects are included in both processes.

In the third panel, we show the allowed region obtained by the full global analysis, where we *simultaneously* include nonstandard effects in detection and in propagation. The effect of including NU couplings in both processes leads to an appreciable reduction of the allowed region evidencing a high complementarity and synergy of the two kinds of constraints, which effectively turns the global allowed region into a ''round'' shape.

It is interesting to observe that the allowed region in the third panel looks like just a naïve combination of the two regions determined *separately* only by detection and only by propagation. This result is important since, *a priori*, one would in principle expect a possible degeneracy among nonstandard effects induced at the level of detection and those induced at the level of propagation. In particular, some region of the parameter space could exist where nonstandard effects in detection could counterbalance those induced in the propagation process (and vice versa). Our analysis shows, *a posteriori*, that such a degeneracy is instead absent. One can qualitatively understand this behavior noting that, although nonstandard propagation effects could in principle partially undo the modifications induced by the nonstandard detection in Super-K, their presence would unavoidably spoil the agreement of *all of the other* experimental results (Cl, Ga, and SNO) with their respective theoretical predictions (which are all well described by standard propagation.)

We close this section quoting the range allowed [at 90% C.L. (2 d.o.f.)] for the amplitude of the nonuniversal R-type coupling of electron neutrinos with electrons,

$$-0.27 < \varepsilon_{ee}^{eR} < 0.59, \tag{12}$$

and for the L-type one,

$$-0.036 < \varepsilon_{ee}^{eL} < 0.063. \tag{13}$$

We observe that our limits are comparable with those found by laboratory experiments [48].

V. CONSTRAINTS ON TAU NEUTRINO INTERACTIONS

In this section, we present the numerical results of the analysis in the presence of nonuniversal couplings of ν_τ with electrons. As in the case of the electron neutrinos presented in the previous section, also in this case we have performed a joint analysis of solar and KamLAND reactor data in the $(\Delta m_{21}^2, \sin^2\theta_{12}, \varepsilon_{\tau\tau}^{eL}, \varepsilon_{\tau\tau}^{eR})$ parameter space, again taking into account that only the vectorial combination of the chiral couplings enters the propagation. In contrast to the case considered in the previous section, for the $\varepsilon_{\tau\tau}^{eL}$ case the analysis is performed for a wider range than considered for ε_{ee}^{eL}, since the current laboratory constraints are too weak to resolve the degeneracy pattern [47].

Note that in the present case the signal observed in the Super-K experiment is the sum of the standard contribution due to scattering of the three neutrino flavors and of an additional nonstandard contribution due to the interaction of τ neutrinos with electrons through the neutral current. These neutrinos originate from solar neutrino oscillations into a state ν_a which we approximate as an equal mixture of ν_μ and ν_τ, corresponding to maximal atmospheric mixing angle and zero θ_{13}.

Figure 3 is analogous to Fig. 2 but with the three panels showing, respectively, the regions allowed in the $[\varepsilon_{\tau\tau}^{eL}, \varepsilon_{\tau\tau}^{eR}]$ plane. Notice that in this case the scale of the L-type coupling is different from the case of electron neutrinos, being almost an order of magnitude larger. In the first panel, the ''two-island'' behavior is a manifestation of the degeneracy pattern which exists for the electron case [47] and which is not fully lifted by our current global analysis. It is clear from Eq. (11) that the neutrino-electron cross section is symmetric under the simultaneous transformation $g_1^a \to -g_1^a$ and $g_2^a \to -g_2^a$. Moreover, the last term, already small due to the ratio m_e/E_ν, is further suppressed compared with the electron neutrino case since its coefficient $g_1^\tau g_2^\tau$ is now smaller. Therefore, there is

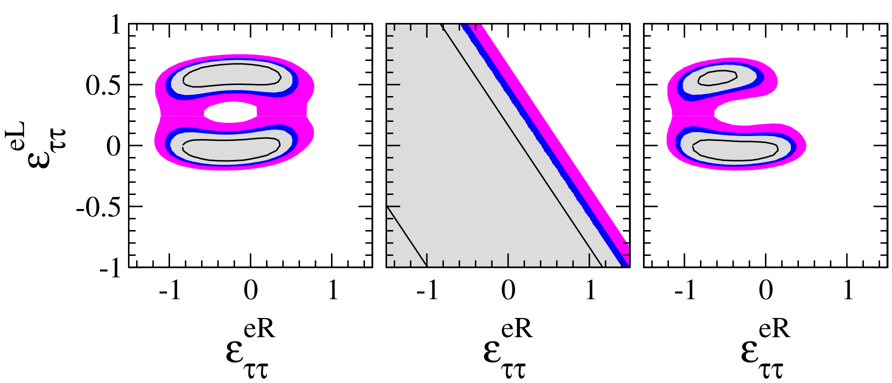

FIG. 3 (color online). Constraints on the τ neutrino nonstandard interactions. Bounds at 68%, 90%, 95%, and 99% for 2 d.o.f. In the left panel nonstandard effects are included only in the detection, in the middle panel only in propagation, and in the right panel the effects are included in both processes. Notice the different scale for the left coupling with respect to the case of electron neutrinos presented in Fig. 2.

actually an approximate symmetry under separate changes in the sign of $g^a_{1,2}$. In our case this can be achieved by setting, for instance, $\varepsilon^{eL}_{\tau\tau} = -2g^\tau_1 \simeq 0.54$, which effectively amounts to the transformation $\tilde{g}^\tau_1 = g^\tau_1 + \varepsilon^{eL}_{\tau\tau} \rightarrow -g^\tau_1$. As can be seen in Fig. 3, our global data analysis is already able to resolve this degeneracy at 99% C.L. but is not able to resolve the same degeneracy for the $\varepsilon^{eR}_{\tau\tau}$ case. As in the case of interaction with electron neutrinos treated in the previous section, we find that the barycenter of the allowed region is slightly shifted toward negative values of the L-type parameter, again indicating a weak preference for an energy-independent differential cross section (see comments in Sec. IV).

In the middle panel, we show the constraints obtained including nonstandard effects only in propagation. We observe that in this case [see Eq. (7)] we have $\varepsilon^{eV}_{\tau\tau} = \varepsilon'/\sin^2\theta_{23} \simeq 2\varepsilon'$, explaining the reduced sensitivity to the vectorial coupling. Finally, the right panel is obtained, as before, by consistently including nonstandard effects both in neutrino detection as well as in propagation. As for the case of electron neutrinos discussed in Sec. IV, the full analysis clearly shows the complementarity among the constraints coming from detection and propagation and the absence of any possible degeneracy between the two effects. We find the following 90% C.L. (2 d.o.f.) allowed range of the nonstandard amplitude of R-type coupling:

$$-1.05 < \varepsilon^{eR}_{\tau\tau} < 0.31, \tag{14}$$

while two disjoint ranges for the L-type coupling are obtained:

$$-0.16 < \varepsilon^{eL}_{\tau\tau} < 0.11, \qquad 0.41 < \varepsilon^{eL}_{\tau\tau} < 0.66, \tag{15}$$

corresponding to the "two-island" region discussed above. We observe that also in this case our limits are comparable to the existing laboratory bounds [48].

VI. SUMMARY AND CONCLUSIONS

Motivated by neutrino mass extensions of the standard electroweak model that imply the existence of neutrino nonstandard interactions, we have considered the constraints on the strength of effective nonuniversal flavor-conserving four-fermion operators $\nu_\alpha \nu_\alpha \bar{e} e$ with electrons, where $\alpha = e, \tau$, that can be obtained from solar and reactor (KamLAND) neutrino data. We have consistently taken into account the effect of nonstandard physics both at the level of neutrino propagation, where they modify the standard MSW behavior, as well as at the level of detection, where they affect the cross section of neutrino elastic scattering on electrons.

Our analysis allows us to trace the following important conclusions: (I) The constraints on NU couplings obtained by detection and propagation of solar neutrinos are of comparable sensitivity. (II) The constraints coming from the two processes are highly complementary, and the general analysis allows considerable restrictions of the parameter space. (III) The current data seem powerful enough to remove degeneracies possibly arising among NU couplings at the level of detection and propagation, respectively. (IV) The limits we find are comparable with those found by means of other model-dependent searches.

ACKNOWLEDGMENTS

This work was supported by Spanish Grants No. FPA2008-00319/FPA and No. FPA2008-01935-E/FPA and ILIAS/N6 Contract No. RII3-CT-2004-506222. M. A. T. is supported by the DFG (Germany) under Grant No. SFB-676. A. B. and O. G. M. were supported by Conacyt and the HELEN program.

[1] L. Wolfenstein, Phys. Rev. D **17**, 2369 (1978).
[2] S. P. Mikheev and A. Y. Smirnov, Sov. J. Nucl. Phys. **42**, 913 (1985).
[3] B. T. Cleveland *et al.*, Astrophys. J. **496**, 505 (1998).
[4] Y. Fukuda *et al.* (Kamiokande Collaboration), Phys. Rev. Lett. **77**, 1683 (1996).
[5] J. N. Abdurashitov *et al.* (SAGE Collaboration), J. Exp. Theor. Phys. **95**, 181 (2002).
[6] W. Hampel *et al.* (GALLEX Collaboration), Phys. Lett. B **447**, 127 (1999).
[7] M. Altmann *et al.* (GNO Collaboration), Phys. Lett. B **616**, 174 (2005).
[8] R. L. Hahn, in Proceedings of the Neutrino 2008 Conference, Christchurch, New Zealand, 2008 (unpublished).
[9] V. Gavrin, in Proceedings of the Neutrino 2006 Conference, Santa Fe, New Mexico, 2006 (unpublished).
[10] S. Fukuda *et al.* (Super-Kamiokande Collaboration), Phys. Rev. Lett. **86**, 5651 (2001).
[11] S. Fukuda *et al.* (Super-Kamiokande Collaboration), Phys. Rev. Lett. **86**, 5656 (2001).
[12] S. Fukuda *et al.* (Super-Kamiokande Collaboration), Phys. Lett. B **539**, 179 (2002).
[13] M. B. Smy *et al.* (Super-Kamiokande Collaboration), Phys. Rev. D **69**, 011104 (2004).
[14] Q. R. Ahmad *et al.* (SNO Collaboration), Phys. Rev. Lett. **87**, 071301 (2001).
[15] Q. R. Ahmad *et al.* (SNO Collaboration), Phys. Rev. Lett. **89**, 011301 (2002).
[16] Q. R. Ahmad *et al.* (SNO Collaboration), Phys. Rev. Lett. **89**, 011302 (2002).
[17] S. N. Ahmed *et al.* (SNO Collaboration), Phys. Rev. Lett. **92**, 181301 (2004).
[18] B. Aharmim *et al.* (SNO Collaboration), Phys. Rev. C **72**,

055502 (2005).
[19] B. Aharmim *et al.* (SNO Collaboration), Phys. Rev. Lett. **101**, 111301 (2008).
[20] C. Arpesella *et al.* (Borexino Collaboration), Phys. Lett. B **658**, 101 (2008).
[21] C. Arpesella *et al.* (Borexino Collaboration), Phys. Rev. Lett. **101**, 091302 (2008).
[22] G. Bellini *et al.* (Borexino Collaboration), arXiv:0808.2868.
[23] K. Eguchi *et al.* (KamLAND Collaboration), Phys. Rev. Lett. **90**, 021802 (2003).
[24] T. Araki *et al.* (KamLAND Collaboration), Phys. Rev. Lett. **94**, 081801 (2005).
[25] S. Abe *et al.* (KamLAND Collaboration), Phys. Rev. Lett. **100**, 221803 (2008).
[26] G. L. Fogli, E. Lisi, A. Marrone, and A. Palazzo, Prog. Part. Nucl. Phys. **57**, 742 (2006).
[27] M. Maltoni, T. Schwetz, M. A. Tortola, and J. W. F. Valle, New J. Phys. **6**, 122 (2004).
[28] T. Schwetz, M. Tortola, and J. W. F. Valle, New J. Phys. **10**, 113011 (2008); previous works by other groups as well as the relevant experimental references are given therein.
[29] G. L. Fogli *et al.*, Phys. Rev. D **78**, 033010 (2008).
[30] A. Schaefer and S. E. Koonin, Phys. Lett. B **185**, 417 (1987);
[31] P. I. Krastev and A. Y. Smirnov, Mod. Phys. Lett. A **6**, 1001 (1991).
[32] F. N. Loreti and A. B. Balantekin, Phys. Rev. D **50**, 4762 (1994);
[33] H. Nunokawa, A. Rossi, V. B. Semikoz, and J. W. F. Valle, Nucl. Phys. **B472**, 495 (1996).
[34] C. P. Burgess, N. S. Dzhalilov, T. I. Rashba, V. B. Semikoz, and J. W. F. Valle, Mon. Not. R. Astron. Soc. **348**, 609 (2004).
[35] C. Burgess *et al.*, Astrophys. J. **588**, L65 (2003).
[36] C. P. Burgess *et al.*, J. Cosmol. Astropart. Phys. 01 (2004) 007.
[37] G. L. Fogli, E. Lisi, A. Marrone, D. Montanino, and A. Palazzo, Phys. Rev. D **76**, 033006 (2007).
[38] O. G. Miranda *et al.*, Nucl. Phys. **B595**, 360 (2001).
[39] O. G. Miranda, T. I. Rashba, A. I. Rez, and J. W. F. Valle, Phys. Rev. Lett. **93**, 051304 (2004); Phys. Rev. D **70**, 113002 (2004).
[40] J. Schechter and J. W. F. Valle, Phys. Rev. D **24**, 1883 (1981); **25**, 283(E) (1982).
[41] E. K. Akhmedov, Phys. Lett. B **213**, 64 (1988).
[42] S. Pakvasa and J. W. F. Valle, Proc. Indian Natl. Sci. Acad., Part A **70**, 189 (2004).
[43] Z. Berezhiani, R. S. Raghavan, and A. Rossi, Nucl. Phys. **B638**, 62 (2002).
[44] S. Davidson, C. Pena-Garay, N. Rius, and A. Santamaria, J. High Energy Phys. 03 (2003) 011.
[45] A. Friedland, C. Lunardini, and C. Pena-Garay, Phys. Lett. B **594**, 347 (2004).
[46] M. M. Guzzo, P. C. de Holanda, and O. L. G. Peres, Phys. Lett. B **591**, 1 (2004).
[47] J. Barranco, O. G. Miranda, C. A. Moura, and J. W. F. Valle, Phys. Rev. D **73**, 113001 (2006).
[48] J. Barranco, O. G. Miranda, C. A. Moura, and J. W. F. Valle, Phys. Rev. D **77**, 093014 (2008).
[49] N. Fornengo, M. Maltoni, R. Tomas Bayo, and J. W. F. Valle Phys. Rev. D **65**, 013010 (2001).
[50] A. Friedland, C. Lunardini, and M. Maltoni, Phys. Rev. D **70**, 111301(R) (2004).
[51] P. Huber, T. Schwetz, and J. W. F. Valle, Phys. Rev. Lett. **88**, 101804 (2002).
[52] P. Huber, T. Schwetz, and J. W. F. Valle, Phys. Rev. D **66**, 013006 (2002).
[53] P. Huber and J. W. F. Valle, Phys. Lett. B **523**, 151 (2001).
[54] N. C. Ribeiro *et al.*, J. High Energy Phys. 12 (2007) 002.
[55] J. Kopp, M. Lindner, T. Ota, and J. Sato, arXiv:0710.1867.
[56] J. Kopp, T. Ota, and W. Winter, Phys. Rev. D **78**, 053007 (2008).
[57] A. Esteban-Pretel, J. W. F. Valle, and P. Huber, Phys. Lett. B **668**, 197 (2008).
[58] O. G. Miranda, M. A. Tortola, and J. W. F. Valle, J. High Energy Phys. 10 (2006) 008.
[59] J. Schechter and J. W. F. Valle, Phys. Rev. D **22**, 2227 (1980).
[60] P. Minkowski, Phys. Lett. **67B**, 421 (1977).
[61] M. Gell-Mann, P. Ramond, and R. Slansky, CERN Print-80-0576, 1979.
[62] T. Yanagida, in *KEK Lectures*, edited by A. Sawada and A. Sugamoto (KEK, Tsukuba, 1979).
[63] R. N. Mohapatra and G. Senjanovic, Phys. Rev. Lett. **44**, 912 (1980).
[64] J. Schechter and J. W. F. Valle, Phys. Rev. D **25**, 774 (1982).
[65] P.-H. Gu, M. Hirsch, U. Sarkar, and J. W. F. Valle, arXiv:0811.0953.
[66] R. N. Mohapatra and J. W. F. Valle, Phys. Rev. D **34**, 1642 (1986).
[67] M. C. Gonzalez-Garcia and J. W. F. Valle, Phys. Lett. B **216**, 360 (1989).
[68] J. Bernabeu *et al.*, Phys. Lett. B **187**, 303 (1987).
[69] G. C. Branco, M. N. Rebelo, and J. W. F. Valle, Phys. Lett. B **225**, 385 (1989).
[70] N. Rius and J. W. F. Valle, Phys. Lett. B **246**, 249 (1990).
[71] J. W. F. Valle, Phys. Lett. B **199**, 432 (1987).
[72] H. Nunokawa, Y. Z. Qian, A. Rossi, and J. W. F. Valle, Phys. Rev. D **54**, 4356 (1996).
[73] A. Esteban-Pretel, R. Tomas, and J. W. F. Valle, Phys. Rev. D **76**, 053001 (2007).
[74] L. J. Hall and M. Suzuki, Nucl. Phys. **B231**, 419 (1984).
[75] G. G. Ross and J. W. F. Valle, Phys. Lett. **151B**, 375 (1985).
[76] J. R. Ellis *et al.*, Phys. Lett. **150B**, 142 (1985).
[77] A. Santamaria and J. W. F. Valle, Phys. Lett. B **195**, 423 (1987).
[78] M. A. Diaz, J. C. Romao, and J. W. F. Valle, Nucl. Phys. **B524**, 23 (1998).
[79] M. Hirsch, M. A. Diaz, W. Porod, J. C. Romao, and J. W. F. Valle, Phys. Rev. D **62**, 113008 (2000); **65**, 119901(E) (2002).
[80] A. Abada, S. Davidson, and M. Losada, Phys. Rev. D **65**, 075010 (2002).
[81] M. A. Diaz, M. Hirsch, W. Porod, J. C. Romao, and J. W. F. Valle, Phys. Rev. D **68**, 013009 (2003).
[82] V. D. Barger, G. F. Giudice, and T. Han, Phys. Rev. D **40**, 2987 (1989).
[83] K. S. Babu, Phys. Lett. B **203**, 132 (1988).
[84] A. Zee, Phys. Lett. **93B**, 389 (1980).

[85] M. B. Gavela, D. Hernandez, T. Ota, and W. Winter, Phys. Rev. D **79**, 013007 (2009).
[86] S. Antusch, J. P. Baumann, and E. Fernandez-Martinez, Nucl. Phys. **B810**, 369 (2009).
[87] S. Bergmann and A. Kagan, Nucl. Phys. **B538**, 368 (1999).
[88] M. C. Gonzalez-Garcia *et al.*, Phys. Rev. Lett. **82**, 3202 (1999).
[89] M. M. Guzzo, A. Masiero, and S. T. Petcov, Phys. Lett. B **260**, 154 (1991).
[90] E. Roulet, Phys. Rev. D **44**, R935 (1991).
[91] C. Amsler *et al.* (Particle Data Group), Phys. Lett. B **667**, 1 (2008).
[92] J. N. Bahcall, A. M. Serenelli, and S. Basu, Astrophys. J. Suppl. Ser. **165**, 400 (2006).
[93] A. Y. Smirnov, arXiv:hep-ph/0702061.
[94] G. L. Fogli, E. Lisi, A. Marrone, and A. Palazzo, Phys. Lett. B **583**, 149 (2004).
[95] J. N. Bahcall, M. Kamionkowski, and A. Sirlin, Phys. Rev. D **51**, 6146 (1995).